DOI: https://doi.org/10.33103/uot.ijccce.18.2.2

H_2 Sliding Mode Controller Design for Mobile Inverted Pendulum System

Hazem I. Ali[1], Mustafa J. Kadhim[2]
[1,2]Control and Systems Eng. Dept. at University of Technology
60143@uotechnology.edu.iq, cse.60034@uotechnology.edu.iq

Abstract— *The design of an H_2 sliding mode controller for a mobile inverted pendulum system is proposed in this paper. This controller is conducted to stabilize the mobile inverted pendulum in the upright position and drive the system to a desired position. Lagrangian approach is used to develop the mathematical model of the system. The H_2 controller is combined with the sliding mode control to give a better performance compared to the case of using each of the above controllers alone. The results show that the proposed controller can stabilize the system and drive the output to a given desired input. Furthermore, variations in system parameters and disturbance are considered to illustrate the robustness of the proposed controller.*

Index Terms— *H_2 statefeedback, Optimal control, Mobile inverted pendulum system, Robust control, Sliding mode control.*

I. INTRODUCTION

Mobile inverted pendulum system has been considered as a typical problem of nonlinear systems. Several practical systems have been implemented according to the mobile inverted pendulum system, such as the Segway, the Legway, the JOE and the Nbot, etc [1]. Human body can simply be represented as a mobile inverted pendulum system balancing by walking. Balance control is an important subject in robotics and control [2]. There are two control problems in the mobile inverted pendulum system, which are stabilizing and tracking [3]. The system is an underactuated that makes a challenge to stabilize the system with an acceptable time response specification and disturbance rejection. On the other hand, the uncertainty in the system model parameter causes a variation in system dynamics [4, 5].

There are many control strategies for controlling the mobile inverted pendulum system. Noh et al. [6] in 2009 proposed a radial basis function network as an auxiliary controller to help the PID controllers for mobile inverted pendulum. The back propagation algorithm has been developed for the radial basis function network of the mobile inverted pendulum system. Moghavvemi et al. [7] in 2010 applied an explicit model predictive controller to stabilize an inverted pendulum system. Explicit solutions to constrained linear model predictive controller were computed by solving multi-parametric quadratic programs. Adhikary and Mahanta [8] in 2013 presented an integral backstepping sliding mode to stabilize and swing up a pendulum on the cart system. Ben Mansour et al. [9] in 2016 proposed a control architecture for the mobile inverted pendulum based on two layers. A speed inner loop control scheme was designed based on the state feedback technique to stabilize the inverted structure of the robot. A second outer loop control scheme was proposed to help the robot navigate along any desired path. Odry et al. [10] in 2015 applied the linear-quadratic-Gaussian control for a two-wheeled mobile inverted pendulum. Mu et

Received 6 Feb 2018; Accepted 9 May 2018
 ISSN (Print) 1811-9212 ISSN (Online) 2617-3352

al. [11] in 2017 presented a nonlinear sliding mode control to stabilize a two-wheeled mobile robot system and drive it into the desired trajectory.

The main objective of this paper is to obtain a new robust and optimal controller that achieves a more desirable performance. The goal can be achieved by combining the H_2 control with the sliding mode control. The model of the mobile inverted pendulum is adopted by Euler Lagrange equation of motion methods. The design of H_2 sliding mode controller is presented to achieve an optimal performance in presence of system parameter variation and disturbance signals.

II. SYSTEM MATHEMATICAL MODEL

The mobile inverted pendulum components are: chassis, DC motors, inverted pendulum, two wheels and control unit. The system chassis supports the wheels and the pendulum. The DC motors rotate the wheels with respect to the chassis. The system control unit controls the DC motors to move the system [12]. The overall system structure is given in Fig. 1. Euler Lagrange method is used to obtain the mathematical model of the mobile inverted pendulum system.

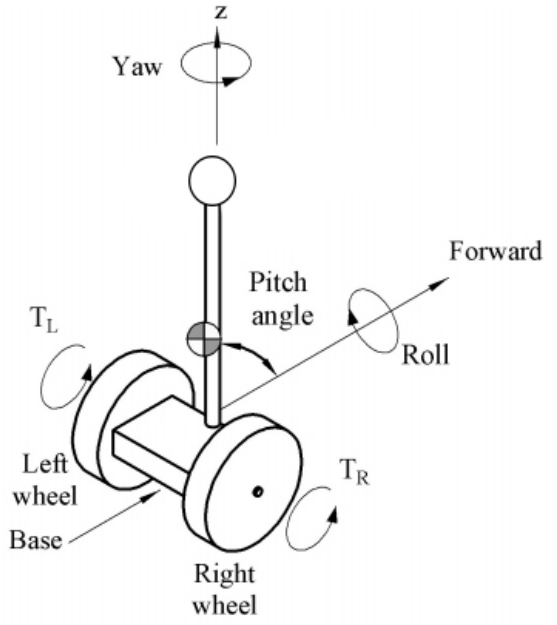

FIG. 1. THE MOBILE INVERTED PENDULUM SYSTEM STRUCTURE [13].

As shown in Fig. 1, the system has three degrees of freedom on the three axes. Roll represents a rotation around the lateral axis X, pitch represents a rotation around the vertical axis Y and the yaw represents a rotation around the lateral axis Z. Fig. 2 illustrates the schematic structure of the system.

The Lagrangian function is given by:

$$L = E - V \tag{1}$$

The Euler Lagrange equation can be described by:

$$\frac{\partial}{\partial t}\left(\frac{\partial L}{\partial \dot{q}}\right) - \frac{\partial L}{\partial q} = F_i \tag{2}$$

The total kinetic energy is given by:

$$E=E_B^{Tra} + E_B^{Rot} + E_W^{Tra} + E_W^{Rot} \tag{3}$$

Received 6 Feb 2018; Accepted 9 May 2018
 ISSN (Print) 1811-9212 ISSN (Online) 2617-3352

The linear torque for the body is:

$$E_B^{Tra} = \frac{1}{2} M_b \left[\dot{x}^2 + 2h\,\dot{x}\,\dot{\phi}\,cos\phi + h^2\,\dot{\phi}^2 + h^2\,\dot{\psi}^2 \sin^2\phi\right] \quad (4)$$

The rotation torque for the body is:

$$E_B^{Rot} = \frac{1}{2}\ [I_x\dot{\phi}^2 + I_y\dot{\psi}^2 sin^2\phi + I_z\dot{\psi}^2 cos^2\phi] \quad (5)$$

The rotation torque for the wheel is:

$$E_W = \frac{1}{2}\ (M_w + \frac{I_a}{R^2})\ (\dot{x}^2 + l\,\dot{\psi}^2) \quad (6)$$

Total potential energy V is;

$$V = M_b g h\ cos\phi + M_w\ g\ R \quad (7)$$

The total energy L is given by:

$$L = \left[\frac{M_b}{2} + M_w + \frac{I_a}{R^2}\right]\dot{x}^2 + \left[M_b h^2 + \frac{1}{2}I_x\right]\dot{\phi}^2\dot{\psi}^2 + M_b h cos\phi\dot{x}\dot{\phi}\ - [M_b g h cos\phi + M_b g R] + \left[\left(M_w + \frac{I_a}{R^2}\right)l^2 + \frac{1}{2}\left(I_y sin^2\phi + I_z cos^2\phi + M_b h sin^2\phi\right)\right] \quad (8)$$

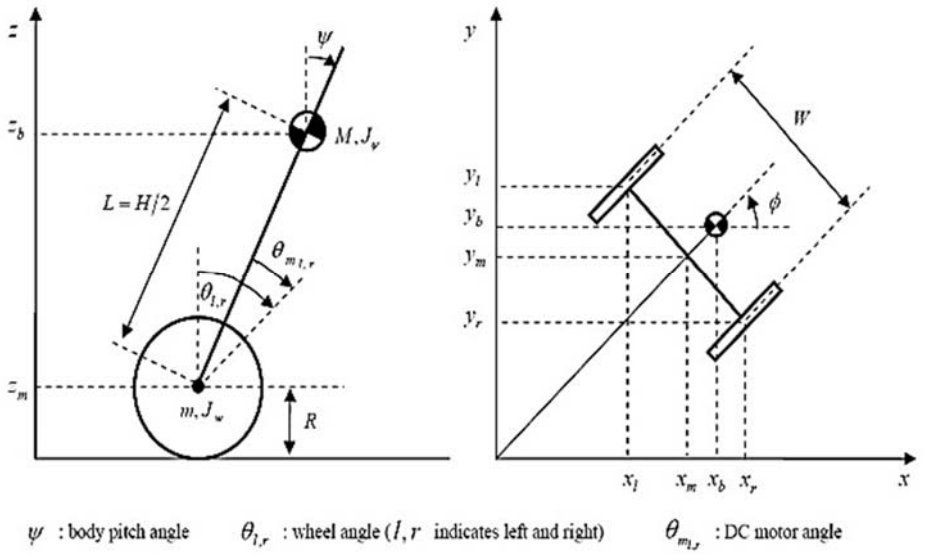

FIG. 2. THE MOBILE INVERTED PENDULUM SYSTEM SCHEMATIC STRUCTURE [14].

By partial differentiation of equation (8) for each of $(\dot{x},\ \dot{\phi},\ \dot{\psi})$ yields:
For x coordinate

$$\ddot{x} = \frac{M_b h R cos\phi\,[M_b h^2 - I_z + I_y] sin\phi cos\phi}{(M_b h^2 + I_x)[(M_b + 2M_w)R^2 + 2I_a] - (M_b R h cos\phi)^2}\dot{\psi}^2 + \frac{R^2(M_b h^2 + I_x)M_b h sin\phi}{(M_b h^2 + I_x)[(M_b + 2M_w)R^2 + 2I_a] - (M_b R h cos\phi)^2}\dot{\phi}^2 - \frac{M_b^2 g R^2 h^2 sin\phi cos\phi}{(M_b h^2 + I_x)[(M_b + 2M_w)R^2 + 2I_a] - (M_b R h cos\phi)^2} + \frac{R(M_b h^2 + M_b h R cos\phi + I_x)}{(M_b h^2 + I_x)[(M_b + 2M_w)R^2 + 2I_a] - (M_b R h cos\phi)^2}\ (T_1 + T_2) \quad (9)$$

For ϕ coordinate

$$\ddot{\phi} = \frac{[M_b R^2 + 2M_w R^2 + 2I_a][M_b h^2 - I_z + I_y] sin\phi cos\phi}{(R h M_b sin\phi)^2 + [(M_b + 2M_w)R^2 + 2I_a]I_x + 2M_b h^2(M_w R^2 + I_a)}\dot{\psi}^2\ - \frac{[M_b R^2 + 2M_w R^2 + 2I_a]M_b h R cos\phi}{(R h M_b sin\phi)^2 + [(M_b + 2M_w)R^2 + 2I_a]I_x + 2M_b h^2(M_w R^2 + I_a)}\ (T_1 + T_2)$$

Received 6 Feb 2018; Accepted 9 May 2018
 ISSN (Print) 1811-9212 ISSN (Online) 2617-3352

$$-\frac{M_b^2R^2h^2sin\phi cos\phi}{(RhM_bsin\phi)^2+[(M_b+2M_w)R^2+2I_a]I_x+2M_bh^2(M_wR^2+I_a)}\dot{\phi}^2+\frac{[M_bR^2+2M_wR^2+2I_a]M_bhgsin\phi}{(RhM_bsin\phi)^2+[(M_b+2M_w)R^2+2I_a]I_x+2M_bh^2(M_wR^2+I_a)} \quad (10)$$

For ψ coordinate,

$$\ddot{\psi}=\frac{l}{R\left[2\left(M_w+\frac{I_a}{R^2}\right)l^2+I_y\sin^2\phi+I_z cos^2\phi+M_bh^2sin\phi\right]}(T_1-T_2)-\frac{2[M_bh^2+I_y-I_z]\cos\phi\sin\phi\dot{\psi}\dot{\phi}}{R\left[2\left(M_w+\frac{I_a}{R^2}\right)l^2+I_y\sin^2\phi+I_z cos^2\phi+M_bh^2sin\phi\right]} \quad (11)$$

The Jacobian linearization method is used to obtain the system linearized model of the mobile inverted pendulum system. The resulted model is:

$$\frac{dx(t)}{dt}=f(x(t),T) \quad (12)$$

where:

$$x(t)=\begin{bmatrix}x\\ \dot{x}\\ \psi\\ \dot{\psi}\\ \phi\\ \dot{\phi}\end{bmatrix} \quad (13)$$

The Jacobian equation is applied for the system with equilibrium points (X_0, T_0) defined as:

$$X_0=(x_0,\dot{x}_0,\psi_0,\dot{\psi}_0,\phi_0,\dot{\phi}_0)=(0,0,0,0,0,0) \quad (14)$$

$$T_0=0 \quad (15)$$

By using Matlab, equations (9), (10) and (11) become:

$$\ddot{\phi}(t)=\frac{[M_bR^2+2M_wR^2+2I_a]M_bgh}{[(M_b+2M_w)R^2+2I_a]I_x+2M_bh^2(M_wR^2+I_a)}\phi(t)-\frac{[M_bR^2+2M_wR^2+2I_a]+M_bhR}{[(M_b+2M_w)R^2+2I_a]I_x+2M_bh^2(M_wR^2+I_a)}(T_1+T_2) \quad (16)$$

$$\ddot{x}(t)=-\frac{M_b^2gR^2h^2}{(M_bh^2+I_x)[(M_b+2M_w)R^2+2I_a]-(M_bRh)^2}\phi(t)+\frac{R(M_bh^2+M_bhR+I_x)}{(M_bh^2+I_x)[(M_b+2M_w)R^2+2I_a]-(M_bRh)^2}(T_1+T_2) \quad (17)$$

$$\ddot{\psi}(t)=\frac{l}{R\left[2\left(M_w+\frac{I_a}{R^2}\right)l^2+I_z\right]}(T_1-T_2) \quad (18)$$

Then, the final model is:

$$\begin{bmatrix}\dot{x}(t)\\ \ddot{x}(t)\\ \dot{\psi}(t)\\ \ddot{\psi}(t)\\ \dot{\phi}(t)\\ \ddot{\phi}(t)\end{bmatrix}=\begin{bmatrix}0&1&0&0&0&0\\ 0&0&0&0&a_1&0\\ 0&0&0&1&0&0\\ 0&0&0&0&0&0\\ 0&0&0&0&0&1\\ 0&0&0&0&a_2&0\end{bmatrix}\begin{bmatrix}x(t)\\ \dot{x}(t)\\ \psi(t)\\ \dot{\psi}(t)\\ \phi(t)\\ \dot{\phi}(t)\end{bmatrix}+\begin{bmatrix}0&0\\ b_1&b_2\\ 0&0\\ b_3&-b_4\\ 0&0\\ -b_5&-b_6\end{bmatrix}\begin{bmatrix}T_1\\ T_2\end{bmatrix} \quad (19)$$

$$\begin{bmatrix}x(t)\\ \psi(t)\\ \phi(t)\end{bmatrix}=\begin{bmatrix}1&0&0&0&0&0\\ 0&0&1&0&0&0\\ 0&0&0&0&1&0\end{bmatrix}\begin{bmatrix}x(t)\\ \dot{x}(t)\\ \psi(t)\\ \dot{\psi}(t)\\ \phi(t)\\ \dot{\phi}(t)\end{bmatrix}+D\begin{bmatrix}T_1\\ T_2\end{bmatrix} \quad (20)$$

It is shown that the system has the following eigenvalues $\{0, 0, -10.9719, 10.9719, 0, 0\}$, which show that the system is unstable due to the right hand plane pole.

Received 6 Feb 2018; Accepted 9 May 2018

 ISSN (Print) 1811-9212 ISSN (Online) 2617-3352

where:

$$a_1 = -\frac{M_b^2 g R^2 h^2}{(M_b h^2+I_x)[(M_b+2M_w)R^2+2I_a]-(M_b Rh)^2} \quad (21)$$

$$a_2 = \frac{[M_b R^2+2M_w R^2+2I_a]M_b gh}{[(M_b+2M_w)R^2+2I_a]I_x+2M_b h^2(M_w R^2+I_a)} \quad (22)$$

$$b_1 = \frac{R(M_b h^2+M_b hR+I_x)}{(M_b h^2+I_x)[(M_b+2M_w)R^2+2I_a]-(M_b Rh)^2} \quad (23)$$

$$b_2 = \frac{R(M_b h^2+M_b hR+I_x)}{(M_b h^2+I_x)[(M_b+2M_w)R^2+2I_a]-(M_b Rh)^2} \quad (24)$$

$$b_3 = \frac{l}{R\left[2\left(M_w+\frac{I_a}{R^2}\right)l^2+I_z\right]} \quad (25)$$

$$b_4 = \frac{l}{R\left[2\left(M_w+\frac{I_a}{R^2}\right)l^2+I_z\right]} \quad (26)$$

$$b_5 = \frac{[M_b R^2+2M_w R^2+2I_a]+M_b hR}{[(M_b+2M_w)R^2+2I_a]I_x+2M_b h^2(M_w R^2+I_a)} \quad (27)$$

$$b_6 = \frac{[M_b R^2+2M_w R^2+2I_a]+M_b hR}{[(M_b+2M_w)R^2+2I_a]I_x+2M_b h^2(M_w R^2+I_a)} \quad (28)$$

The nominal values of the real system parameters are listed in Table 1.

TABLE 1. NOMINAL VALUES OF THE SYSTEM PARAMETERS.

Symbol	Value	Unit
M_b	0.502	Kg
M_w	0.054	Kg
h	0.31	m
R	0.065	m
l	0.18	m
I_x	9.1196×10^{-4}	Kgm^2
I_z	6.693×10^{-3}	Kgm^2
I_a	2.851585×10^{-5}	Kgm^2
g	9.81	ms^{-2}

III. CONTROLLER DESIGN

The mobile inverted pendulum model can be expressed as a LTI by:

$$\dot{x}(t) = Ax(t) + B_1\, d(t) + B_2\, u(t) \quad (29)$$

$$e(t) = C_1 x(t) + D_{12}\, u(t) \quad (30)$$

$$y(t) = x(t) \quad (31)$$

Received 6 Feb 2018; Accepted 9 May 2018

 ISSN (Print) 1811-9212 ISSN (Online) 2617-3352

To represent the uncertainty, the uncertain mobile inverted pendulum model can be described by:

$$\dot{x}(t) = Ax(t) + \Delta Ax + B_1\, u(t) + \Delta B_1 u(t) + B_2\, u\,(t) + \Delta B_2\, u(t) + d(t) \qquad (32)$$

where $x(t) \in R^n$ is the state vector, $e(t) \in R^h$ is the output to be controlled vector, $y(t) \in R^r$ is the output, $u(t) \in R^m$ is the control signal vector, $d(t) \in R^t$ is the disturbance, A, B_2 are state space system matrices, B_1 is the disturbance matrix, $\Delta A, \Delta B_1, \Delta B_2$ refer to the matched uncertainty in the matrices A, B_1 , B_2, respectively, and C_1, D_{12} represent the controller design matrices.

The obtaining of a scalar control law is the main objective of this work. The control law is illustrated by:

$$u \;= u_{sw} + u_{eq} \qquad (33)$$

where u_{sw} is the corrective control used to compensate the deviations from the sliding plane. u_{eq} is the equivalent control or the robust control which guarantees that the rate of change of the sliding plane is equal to zero to stay on the sliding surface.

The first part of the control law will be achieved by the unity sliding design, and the second one will be performed using H_2 state feedback controller. A unity sliding mode control strategy for the system is presented in the presence of matched uncertainties and the external disturbance with the mobile inverted pendulum model [16].

From equation (32) which includes the parametric uncertainties and disturbance effect and since the matrix A is not full rank, the singular value decomposition technique (SVD) is used to obtain a full rank matrix then with a controllable pair (A, B) yields:

$$A_o = A - B_2 K \qquad (34)$$

where K is chosen such that the matrix A_o is Hurwitz with the desired close loop roots. Consequently equation (32) becomes:

$$\dot{x}(t) = A_o x(t) + \Delta Ax + B_1 u_o(t) + \Delta B_1 u(t) + B_2 u_o\,(t) + \Delta B_2 u(t) + d(t) \qquad (35)$$

when $u_o(t)$ is the control vector that proved A_o as Hurwitz matrix. Now let the uncertainty in matrices A, B can be written as:

$\Delta A = BA_\delta \;\; and \;\; \Delta B = BB_\delta$

where $A_\delta \in \mathcal{R}^{m\times n}$ and $B_\delta \in \mathcal{R}^{m\times m}$. Then the bracket $\{\Delta Ax + \Delta Bu + d(t)\}$ can be written as:

$$\Delta Ax + \Delta B_1 u + \Delta B_2 u + d(t) = B\{A_\delta x + B_\delta u + \delta(t)\} = B\{(A_\delta - B_\delta K)x + B_\delta u_o + \delta(t)\} \qquad (36)$$

Assuming that the matched uncertainty (A_δ, B_δ) and external disturbance $(\delta(t))$ are bounded, we get

$$\|(A_\delta - B_\delta K)x + B_\delta u_o + \delta(t)\| \le \alpha\|x\| + \beta\|u_o\| + \varepsilon \qquad (37)$$

$$u \;= -\gamma(\|x\|)\frac{S}{\|S\|} - Kx \qquad (38)$$

where

$S = B^T 2Px$ and $\gamma(\|x\|) = \frac{1}{(1-\beta)}\{\alpha\|x\| + \varepsilon + k\}$, $k > 0$

So, the sliding mode control law basically is:

$$u_{sw} = -\gamma(\|x\|)\frac{S}{\|S\|} \qquad (39)$$

For more details about the derivation of equations (34) to (39), the reference [16] can be seen.

Received 6 Feb 2018; Accepted 9 May 2018

 ISSN (Print) 1811-9212 ISSN (Online) 2617-3352

The H_2 control objective is to find a controller that minimizes a quadratic performance index (the H_2 norm) of the system and offers a way of combining the design criteria of quadratic performance and disturbance rejection [13].
For the control system in equations (29),(30) and (31), it is required that the system matrix A is of full rank, the pairs (A, B_1) and (A, B_2) are required to be stabilizable, (C_1, A) is required to be detectable and it is required that all the system state measurements are possible.

Figure 3 presents the block diagram of the full state feedback H_2 control. Assume that

$$M = \begin{bmatrix} A & B_1 & B_2 \\ C & 0 & D_{12} \\ I & 0 & 0 \end{bmatrix} \tag{40}$$

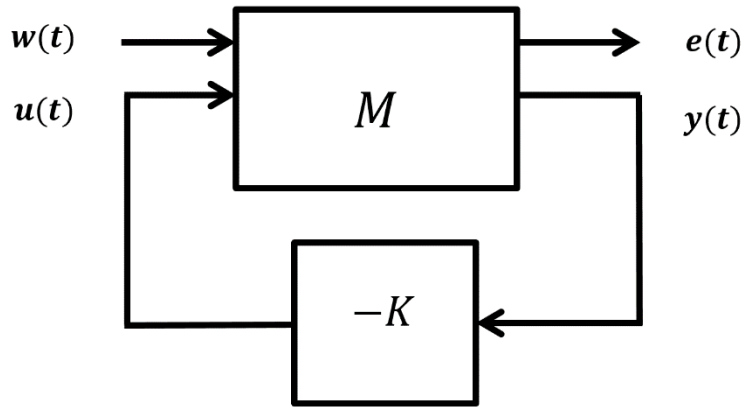

FIG. 3:. $\mathbf{H_2}$ CONTROL STRUCTURE [15].

where $w(t)$ is the exogenous inputs (set point $r(t)$ and disturbance input $d(t)$).The system error for a white noise input can be represented using H_2 norm by:

$$\|T_{ed}\|_{H_2}^2 = E(e^T(t)e(t)) \tag{41}$$

where T_{ed} illustrates the total transfer function from $d(t)$ to $e(t)$, then from equation (30):

$$e^T(t)e(t) = x(t)^T Q_f x(t) + 2x(t)^T N_f u(t) + u(t)^T R_f\, u(t) \tag{42}$$

The minimization of $\|T_{ed}\|_{H_2}^2$ is equivalent to the stochastic regulator problem solution by setting: $Q_f = {C_1}^T C_1$, $N_f = {C_1}^T D_{12}$ and $R_f = {D_{12}}^T D_{12}$ then, the cost function to be minimized is [13]:

$$E\left(e^T(t)e(t)\right) = J(x(t), u(t)) = \int_0^\infty [\, x(t)^T Q_f x(t) + 2x(t)^T N_f u(t) + u(t)^T R_f\, u(t)]dt \tag{43}$$

Consequently:

$$J = \int_{t_0}^{t_f} [\, x(t)^T Q_f x(t) + 2x(t)^T N_f u(t) + u(t)^T R_f\, u(t)]dt \tag{44}$$

where $Q_f \in \mathcal{R}^{n\times n}$ is a symmetric positive semidefinite state weighting matrix, $N_f \in \mathcal{R}^{m\times n}$ is a symmetric positive semidefinite state and control weighting matrix and $R_f \in \mathcal{R}^{m\times m}$ is a symmetric positive definite control weighting matrix.

Received 6 Feb 2018; Accepted 9 May 2018
 ISSN (Print) 1811-9212 ISSN (Online) 2617-3352

The optimal control action is:

$$u_{eq} = -K\,x(t) \tag{45}$$

where

$$K = {R_f}^{-1}({B_1}^T P + {N_f}^T) \tag{46}$$

The Riccati equation is:

$$\left(A - B_2 {R_f}^{-1}\,{N_f}^T\right)^T P + P\left(A - B_2 {R_f}^{-1}\,{N_f}^T\right) - P B_2\,{R_f}^{-1}{B_1}^T P + Q_f - N_f\,{R_f}^{-1}{N_f}^T = 0 \tag{47}$$

where K is called the state feedback gain matrix.

IV. RESULTS AND DISCUSSION

The response of the system using sliding mode control is shown in Fig. 4. The response specifications of the system using sliding mode control are: system position and velocity settling time equal to $15\ sec.$ and $14\ sec.$, pendulum angle and velocity settling time equal to, $15\ sec.$ and $10\ sec.$, and the rotating angle and velocity settling time equal to $12\ sec.$ and $4\ sec$. The resulting control signals are shown in Fig. 5. The designed H_2 sliding mode controller has changed the system eigenvalues to $\{-1070.739,\ -733.323,\ -2.273 + 1.784i,\ -2.273\ 1.784i, -1.395, -1.000\}$ and the system states are stable as shown in Fig. 6. The system time response using H_2 sliding mode control can be summarized as system position and velocity settling time which equal to $3\ sec.$ and $2.5\ sec.$, pendulum angle and velocity settling time equal to, $5\ sec.$ and $5\ sec.$, and the rotating angle and velocity settling time equal to $4\ sec.$ and $4\ sec.$ In addition, it is shown that the pendulum angle deviates between -0.92 and $0.35\ \ degree$. The resulting control signals are shown in Fig. 7. It is apparent that a low control effort has been obtained. The resulting state feedback gain matrix which represents the H_2 control part is:

$$\mathrm{K} = \begin{bmatrix} -1.1181 & -1.4113 & 0.7906 & 0.7916 & -5.3592 & -1.2632 \\ -1.1181 & -1.4113 & -0.7906 & -0.7916 & -5.3592 & -1.2632 \end{bmatrix}$$

For robustness test of the proposed controller, a change of ±25% in system parameters is taken. Fig. 8 shows the output response with parameters uncertainty. Fig. 9 shows the output response of the system with a disturbance of 1 N.m at 4.5 second. As can be seen, the proposed controller can compensate the change in system parameters and achieve the desired performance.

Table 2 below presents a performance specification comparison among the IBSMC (Integral Backstepping Sliding Mode Control) [8], the optimal sliding mode control and the H_2 sliding mode controller, to verify the effectiveness of the designed controller. It's obvious that the H_2 sliding mode controller achieved best performance compared with the other results.

Received 6 Feb 2018; Accepted 9 May 2018

 ISSN (Print) 1811-9212 ISSN (Online) 2617-3352

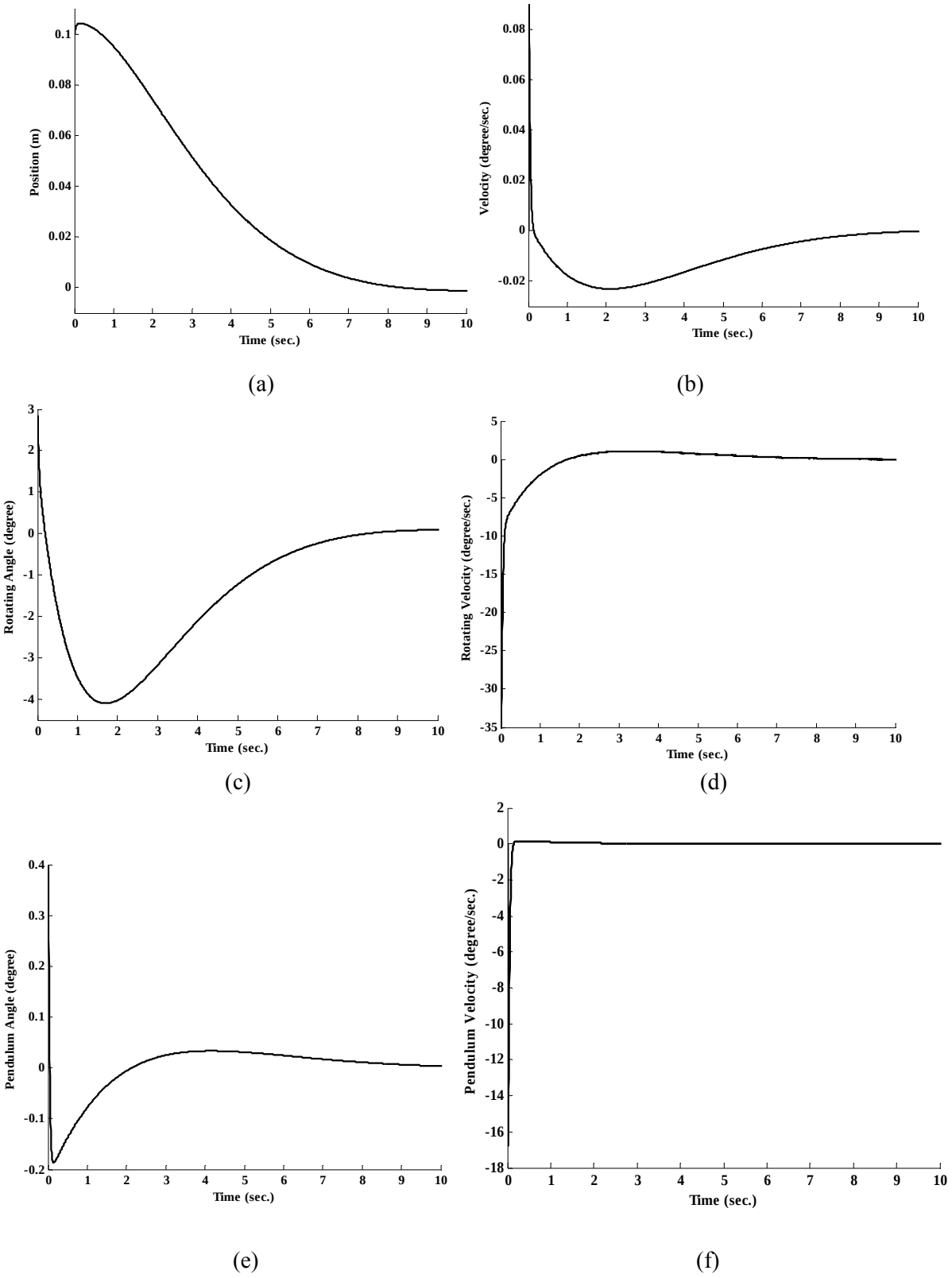

FIG. 4. SLIDING MODE CONTROLLED SYSTEM RESPONSE (A) POSITION (B) VELOCITY (C) ROTATING ANGLE (D) ROTATING VELOCITY (E) PENDULUM ANGLE, (F) PENDULUM VELOCITY.

Received 6 Feb 2018; Accepted 9 May 2018

 ISSN (Print) 1811-9212 ISSN (Online) 2617-3352

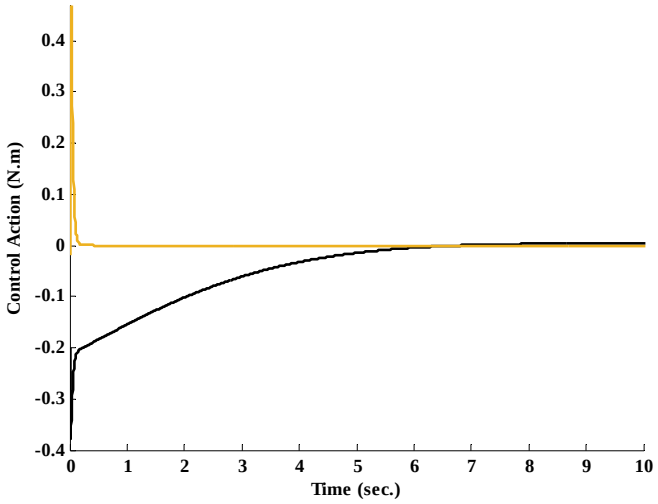

FIG. 5. THE RESULTING CONTROL SIGNALS.

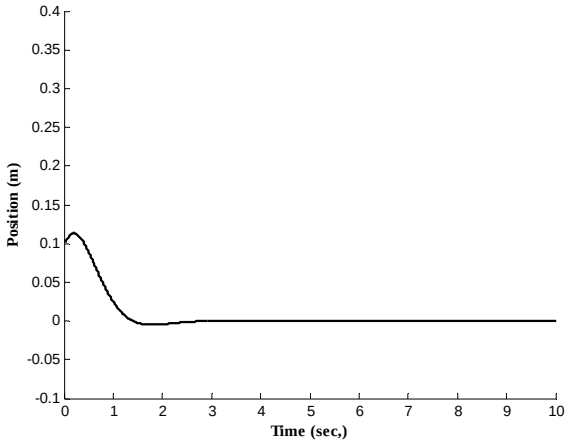

(a)

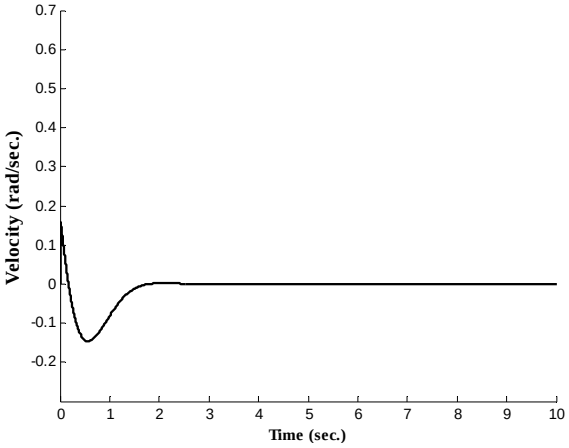

(b)

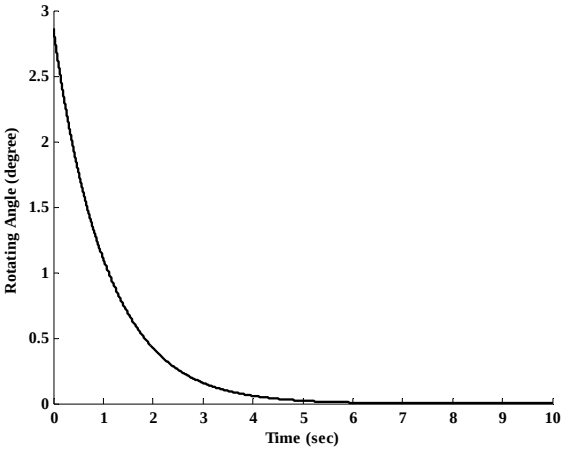

(c)

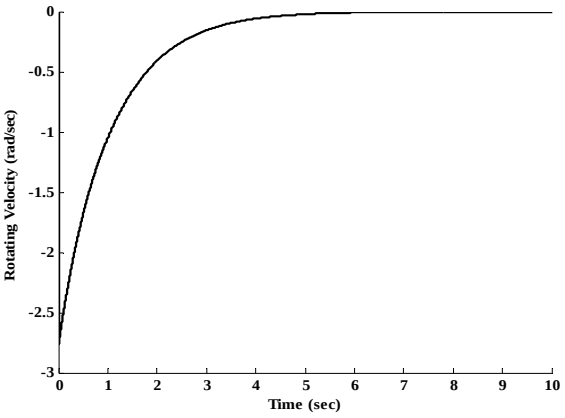

(d)

Received 6 Feb 2018; Accepted 9 May 2018

 ISSN (Print) 1811-9212 ISSN (Online) 2617-3352

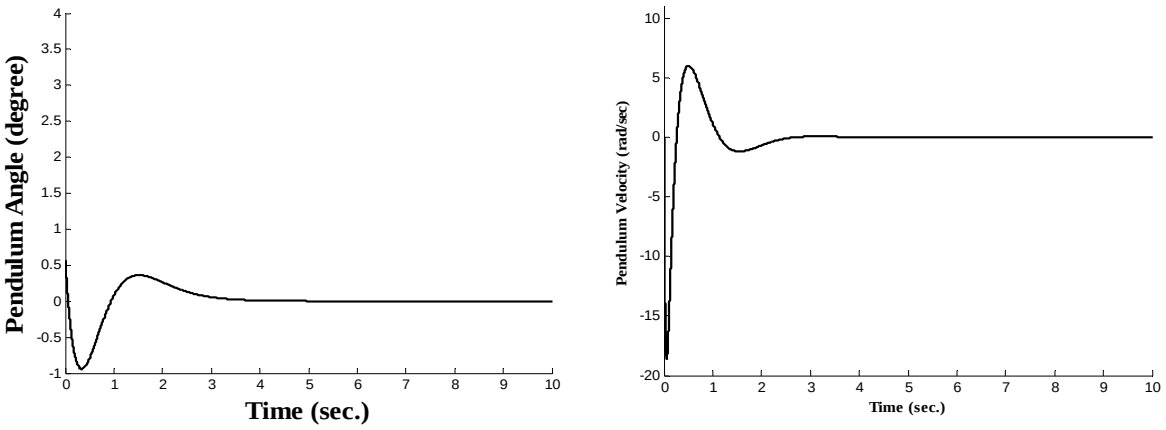

(e) (f)

FIG. 6. H2 SLIDING MODE CONTROLLED SYSTEM RESPONSE (A) POSITION (B) VELOCITY (C) ROTATING ANGLE (D) ROTATING VELOCITY (E) PENDULUM ANGLE, (F) PENDULUM VELOCITY.

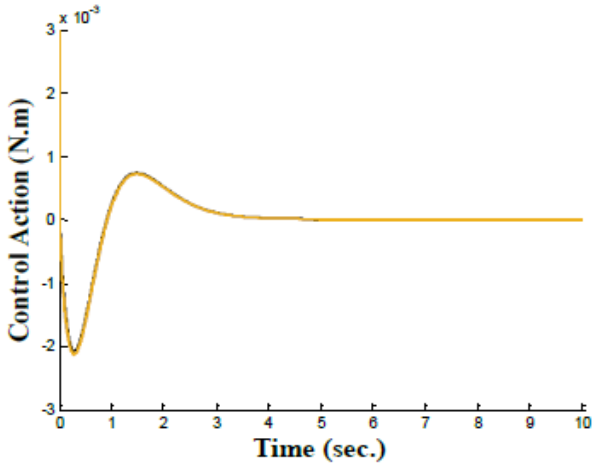

FIG. 7. THE RESULTING CONTROL SIGNALS.

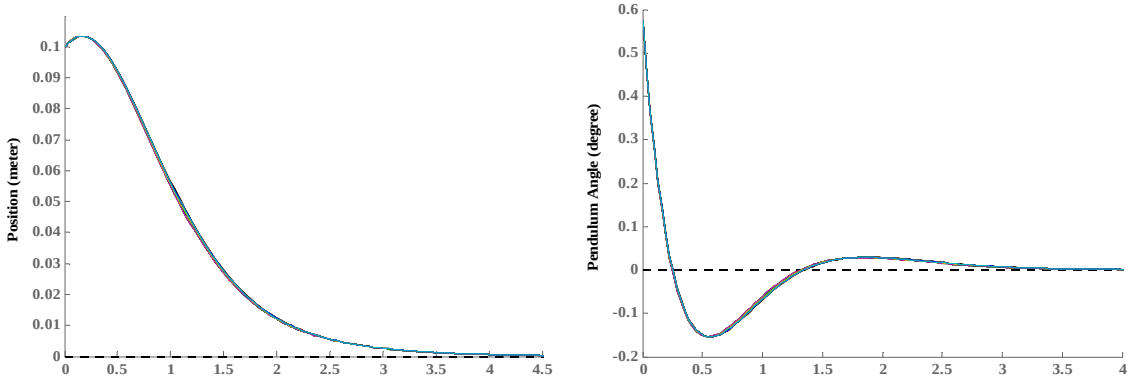

(a) (b)

FIG. 8. CONTROLLED SYSTEM RESPONSE WITH PARAMETERS UNCERTAINTY (A) POSITION, (B) PENDULUM ANGLE.

Received 6 Feb 2018; Accepted 9 May 2018

 ISSN (Print) 1811-9212 ISSN (Online) 2617-3352

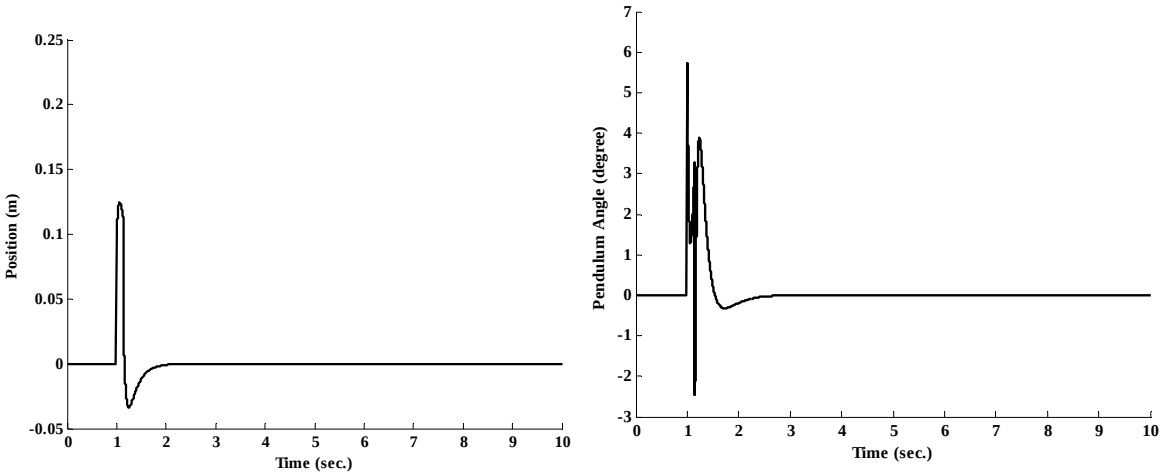

(a) (b)

FIG. 9. CONTROLLED SYSTEM RESPONSE WITH DISTURBANCE (A) POSITION, (B) PENDULUM ANGLE.

Table 2 below presents a performance specification comparison among the IBSMC (Integral Backstepping Sliding Mode Control) [8], the optimal sliding mode control and the H_2 sliding mode controller, to verify the effectiveness of the designed controller. It's obvious that H_2 sliding mode controller achieved best performance compared with the other results.

TABLE 2. COMPARISON AMONG IBSMC, OPTIMAL SLIDING MODE CONTROL AND H2 SLIDING MODE CONTROLLER

Controller	System position			Pendulum angle		
	t_s $(sec.)$	t_r $(sec.)$	M_p $(\%)$	t_s $(sec.)$	t_r $(sec.)$	Deviation $(degree)$
IBSMC	24.421	1.278	6.0205	14.2409	1.8566	-14.33 to 11.3
Optimal SMC	5	1.9	0.2	5	0.2	-1.9 to 2.2
H_2SMC	1.5	0.7	0.18	2.5	0.09	-0.9 to 0.4

V. CONCLUSION

In this paper, the design of an H_2 sliding mode control for a mobile inverted pendulum system has been presented. It was shown that a combination between H_2 control and sliding mode control could achieve a performance better than if only one of them is used. The efficiency of the proposed controller in the presence of system parameter variations and disturbance was proved. Furthermore, it has been shown that the addition of the H_2 controller results in better time response specification and low control effort in comparison to the sliding mode control.

REFERENCES

[1] JH Yoon, JH Park. "Locomotion control of biped robots with serially-linked parallel legs". Transaction of the Korean Soc, Mech. Eng A.; Vol. 34, No. 6, pp.683–693, 2010.

[2] G. H. Lee, S. Jung, "Line Tracking Control of a Two-Wheeled Mobile Robot Using Visual Feedback", International Journal of Advanced Robotic Systems, Vol. 10, No. 3, pp. 1-8, 2013.

[3] A. Al- Jodah, H. Zargarzadeh and M. K. Abbas, "Experimental Verification and Comparison of Different Stabilizing Controllers for a Rotary Inverted Pendulum", IEEE International Conference on Control System, Computing and Engineering, Malaysia, pp.417-423, 2013.

[4] R. Grepl, "Balancing Wheeled Robot: Effective Modelling, Sensory Processing and Simplified Control", Engineering Mechanics, Vol. 16, No. 2, pp.141–154, 2009.

Received 6 Feb 2018; Accepted 9 May 2018

 ISSN (Print) 1811-9212 ISSN (Online) 2617-3352

[5] Y. Takita, H. Date and H. Shimazu, "Competition of Two-wheel Inverted Pendulum Type Robot Vehicle on MCR Course", The IEEE/RSJ International Conference on Intelligent Robots and Systems, pp. 5578-5584, 2009.
[6] J. S. Noh, G. H. Lee, H. J. Choi, and S. Jung, "Robust Control of a Mobile Inverted Pendulum Robot Using a RBF Neural Network Controller", International Conference on Robotics and Biomimetics Bangkok, Thailand, February pp. 21 - 26, 2009.
[7] M. Askari and M. Moghavvemi and H. A. F. Mohamed, "Hard Constraints Explicit Model Predictive Control of an Inverted Pendulum", Iraq J. Electrical and Electronic Engineering, Vol.6 No.1, 2010.
[8] N. Adhikary and C. Mahanta, "Integral backstepping sliding mode control for underactuated systems: Swing-up and stabilization of the Cart–Pendulum System", ISA Transactions, Volume 52, Issue 6, Pages 870-880, 2013,
[9] S. M. Ben Mansour, J. Ghommam and S. M. Naceur, "Design and control of Two-Wheeled Inverted Pendulum Mobile Robot", 3rd International Conference on Automation, Control, Engineering and Computer Science, 2016.
[10] Á. Odry, E. Burkusand and P. Odry, "LQG Control of a Two-Wheeled Mobile Pendulum System", Fourth International Conference on Intelligent Systems and Applications 2015.
[11] J. Mu, X. Yan, and S. Spurgeon, and Z. Mao, "Nonlinear sliding mode control of a two-wheeled mobile robot system", International Journal of Modelling, Identification and Control, Vol 27, No 2, 2017.
[12] K. D. Do and G. Seet, "Motion Control of a Two Wheeled Mobile Vehicle with an Inverted Pendulum", Journal of Intelligent & Robotic Systems, Vol. 60, No. 3, pp. 577-605, 2010.
[13] U. Ali, G. Ufuk and A. Omer, "The Real Time Remote Motion Control of Two Wheeled Mobile Balance Robot by Using Video Streaming", MATEC Web of Conferences 2016.
[14] Y. Kim, S. H. Kim and Y. K. Kwak, "Dynamic Analysis of a Nonholonomic Two-Wheeled Inverted Pendulum Robot", Journal of Intelligent and Robotic Systems 2005.
[15] Y. S. Ban, R. Varatharajoo and M. Ovchinnikov, "H_2 Optimal Control Solution for a Combined Energy and Attitude Control System", Acta Astronautica, Vol. 76, pp. 79-83, 2012.
[16] S. M. Raafat, S. A. Al-Samarraie and A. M. Mahmood, "Unity Sliding Mode Controller Design for Active Magnetic Bearings System", Journal of Engineering, Vol. 21, No. 6, June 2015.

Received 6 Feb 2018; Accepted 9 May 2018

 ISSN (Print) 1811-9212 *ISSN (Online) 2617-3352*